Characteristics of rain-snow transitions over the Canadian Rockies and their changes in warmer climate conditions

Julie M. Thériault, Nicolas R. Leroux, Obert Tchuem Tchuente

Department of Earth and Atmospheric Sciences, Centre ESCER, Université du Québec à Montréal, Montréal, Québec, Canada

Ronald E. Stewart

Department of Environment and Geography, University of Manitoba, Winnipeg, Manitoba, Canada

Corresponding author: Julie M. Thériault, Department of Earth and Atmospheric Sciences, Centre ESCER, Université du Québec à Montréal, Montréal, Canada, theriault.julie@uqam.ca.

Julie M. Thériault: theriault.julie@uqam.ca

Nicolas R. Leroux: leroux.nicolas_romain@courrier.uqam.ca

Obert Tchuem Tchuente : tchuem_tchuente.obert@courrier.uqam.ca

Ronlad E. Stewart : ronald.stewart@umanitoba.ca

Characteristics of rain-snow transitions over the Canadian Rockies and their changes in warmer climate conditions

The southern Canadian Rockies are prone to extreme precipitation that often leads to high streamflow, deep snowpacks, and avalanche risks. Many of these precipitation events are associated with rain–snow transitions, which are highly variable in time and space due to the complex topography. A warming climate will certainly affect these extremes and the associated rain–snow transitions. The goal of this study is to investigate the characteristics and variability of rain–snow transitions aloft and how they will change in the future. Weather Research and Forecasting (WRF) simulations were conducted from 2000 to 2013 and these were repeated but in a warmer pseudo-global warming (PGW) future. Rain–snow transitions occurred aloft throughout the year over the southern Canadian Rockies, but their elevations and depths were highly variable, especially across the continental divide. In PGW conditions, with future air temperatures up to 4–5°C higher on average over the Canadian Rockies, rain–snow transitions are projected to occur more often throughout the year, except during summer. The near-0°C conditions associated with rain–snow transitions are expected to increase in elevation by more than 500 m, resulting in more rain reaching the surface. Overall, this study illustrates the variability of rain–snow transitions, which often impact the location of the snowline. This study also demonstrates the non-uniform changes under PGW conditions, due in part to differences in the types of weather patterns that generate rain–snow transitions across the region.

Keywords: precipitation, convection permitting climate models, mountain meteorology, rain–snow transition, climate change

1. Introduction

The climate in the Canadian Rockies has been rapidly changing for the past 50 years (DeBeer et al., 2016). Although all model projections indicate continued warming, they widely differ regarding precipitation (IPCC, 2021). Understanding future changes in precipitation volumes, rates, timing, and phases is critical because of their impact on snowpacks. In terms of precipitation, its vertical evolution is driven by atmospheric conditions aloft. An increase in the elevation of the 0℃-isotherm aloft will lead to rain at higher elevations and less snow storage during winter. This can alter soil moisture and surface temperature gradients (Minder et al., 2018) leading to a change in precipitation distribution (Wallace & Minder, 2021). This will in turn impact the reach of glaciers and affect the management of water resources such as hydropower and irrigation (e.g. DeBeer et al., 2021).

The Canadian Rockies are prone to extreme precipitation events that can lead to high streamflow, high snowpack variability, and increased avalanche hazards. Given the region’s complex topography (Fig. 1), flooding can be rapid, which increases the risk for communities and industries. The western edge of the Canadian Rockies is also directly affected by atmospheric rivers, which can produce exceptional amounts of precipitation in the region (Radić et al., 2015). Atmospheric rivers are often associated with high temperatures, which raises the likelihood of rain-on-snow events that can lead to avalanches (Hägeli & McClung, 2003) and extreme floods (Guan et al., 2016).

The eastern side of the Canadian Rockies, although associated with a dry climate, can also be subject to extreme precipitation and flooding events. The devastating drought of 1999–2005 (Hanesiak et al., 2011), for example, gave way to saturated conditions that led to the catastrophic flooding in June 2013 that remains one of the most costly natural disasters in Canadian history (Kochtubajda et al., 2016; Pomeroy et al., 2016; Teufel et al., 2017). However, the 2013 event is not unique in the context of modern history: previous floods, such as those in the late 19th and early 20th centuries, rivalled the 2013 event in terms of impact (Flesch & Reuter, 2012; Whitfield & Pomeroy, 2016).

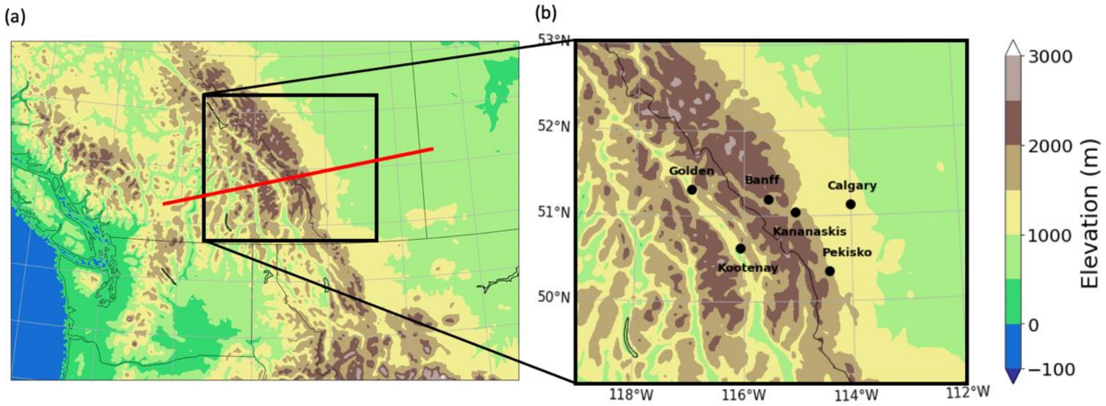

Figure 1. Location of the study area. (a) Domain of the simulations including the topography and the cross section (red line) along which temperature and precipitation were analyzed (Section 5b) and (b) the sub-domain of interest. The meteorological stations used in this study are indicated by the black dots. The elevation of each station and the closest model grid point (in parentheses) are Banff: 1396.9 m (1579.9 m), Calgary: 1081.9 m (1078.2 m), Fernie: 1001.0 m (1199.2 m), Golden: 784.9 m (922.5 m), Kananaskis: 1391.1 m (1474.4 m), Kootenay: 935.0 m (1150.9 m) and Pekisko: 1415.0 m (1509.9 m).

During storms that can last to up to several days, the phase of precipitation can have a strong impact on the severity of flooding. The catastrophic flooding in 2013, which occurred in Alberta, happened in part because precipitation fell as rain at many elevations in the mountainous terrain. This rapidly melted the alpine snowpack and accelerated runoff (Pomeroy et al., 2016). Later in the storm, the elevation of the 0°C-isotherm aloft decreased, leading to snow at the surface, and additional flooding was mitigated because of this phase change.

Spring storms in this region have been studied during atmospheric-related field campaigns in the Kananaskis Valley in Alberta in 2015 (Thériault et al., 2018). During that experiment, 17 storms were documented, and rain, snow, rimed snow, and mixed-phase particles were observed. Solid precipitation was reported at the surface at temperatures up to 8°C due to the dry ambient conditions. This increased the complexity of rain–snow transition analyses because the transition does not necessarily occur at 0°C, as it depends on the relative humidity as well as the type of falling particles (Matsuo & Sayso, 1981a, b). Harder & Pomeroy (2013) showed that using the psychometric equation improves the phase partitioning diagnostic with air temperature over Marmot Creek, near the Kananaskis Valley.

Previous studies have conducted further analyses of the amounts and phases of precipitation that occur across the continental divide. The Storms and Precipitation Across the continental Divide Experiment (SPADE) from April–June 2019 in the Kananaskis Valley documented storms on both sides of the divide simultaneously (Thériault et al., 2022). It was found that rain was observed at the surface almost exclusively on the west side, whereas a mixture of precipitation types was reported on the east. The occurrence of a rain–snow transition is common in mountainous regions, including the Canadian Western Cordillera. For example, Almonte and Stewart (2019) examined surface-related variables and showed that surface rain–snow transitions occurred during 93% of the days in the region from January to April 2010 and that the total hours of occurrence increased by 24% in warmer climate conditions. They also pointed out that the type of associated precipitation, such as the presence of rimed particles, and the sequence of precipitation types can impact the stability of the snowpack and the likelihood of avalanches.

As apparent in the above discussions, the phase of precipitation plays a major role in the severity of storms as well as on the snowpack and in turn, affects water resources. This study examines this issue, and it greatly extends the work of Almonte and Stewart (2019), who studied rain-snow transitions at the surface during a 4-month period, by focusing on rain-snow transitions aloft over a 13-year period. The specific objective of our study is to characterize the rain–snow transitions aloft and the changes that they undergo in a warmer climate over the southern Canadian Rockies. In this study, a rain-snow transition refers to the vertical depth between all snow conditions and all rain conditions. We used the historical and pseudo global warming (PGW) continental United States (CONUS) Weather Research and Forecasting (WRF) simulations at 4 km grid-spacing (Liu et al., 2017). It is difficult to use observations to characterize rain–snow transitions in complex terrain because meteorological stations are sparse. Models can provide more information, especially at higher elevations (Lundquist et al., 2019).

The study is organized as follows. Section 2 describes the methodology used. Section 3 presents the climatology of precipitation amounts and phases, as well as the distribution of precipitation events. Section 4 presents the climatology of the rain–snow transitions in the Canadian Rockies in both historical and warmer climate conditions. Section 5 provides a discussion of the results, and the conclusions are presented in Section 6.

2. Methodology

a. Model simulations

The simulations conducted by Liu et al. (2017) were used in this study. These utilized the WRF model using a 4-km grid-spacing. The control (CTRL) simulation was one-way nested using the 6-h ERA-Interim reanalysis data and for the 1 October 2000 to 30 September 2013 period. A pseudo-global warming (PGW) simulation was conducted to determine the thermodynamic response because of global warming.

Hourly model outputs were provided and used in this study.

For the CTRL simulations, the model was configured using a domain size of 1360 × 1016 grid points with 4-km spacing, covering the continental United States, northern Mexico, and southern Canada. There were 51 vertical levels, extending to 50 hPa. Spectral nudging was used to reproduce past climate conditions as accurately as possible. The Thompson aerosol-aware microphysics scheme was employed in the simulation (Thompson & Eidhammer, 2014). The scheme predicts the mixing ratios of five liquid and ice species: cloud liquid water, rain, cloud ice, snow, and graupel. The scheme also predicts the number concentration for the ice categories.

The PGW approach was used to simulate global warming by perturbing historical weather patterns by adding warmer and moister atmospheric conditions. Liu et al. (2017) applied the 95-year CMIP5 ensemble-mean change signal under the RCP8.5 scenario ($\Delta CMIP5 = \Delta CMIP5_{2071\text{-}2100} - \Delta CMIP5_{1976\text{-}2005}$) on eight physical fields of the ERA-Interim data. The perturbed physical fields were horizontal wind, geopotential, temperature, specific humidity, sea surface temperature, soil temperature, sea level pressure, and sea ice.

These simulations estimate the thermodynamic impact of climate change in a context where the synoptic patterns initiated at the domain boundaries do not change in the future (Shepherd, 2014). Such high-resolution simulations are needed to capture small-scale thermodynamic processes that are crucial for the study of rain–snow transitions, especially in mountainous regions.

b. Evaluation of WRF simulations over the Canadian Rockies

Liu et al. (2017) evaluated the CTRL simulation over the continental United-

States, noting that the 2-m temperature and the surface precipitation were well represented. To gain additional confidence in the model output we have compared the CTRL simulation with additional surface observations over the Canadian Rockies. These are the daily data from six Environment and Climate Change Canada (ECCC) stations over our domain (Fig. 1) and the Daymet (Thornton et al., 2020) product. Daymet is a gridded daily product that interpolates and extrapolates surface observations at 1 km grid-spacing over North America. Daymet provides daily precipitation as well as minimum and maximum air temperatures over North America. It starts in 1980 until the latest full calendar year. SNOTEL precipitation gauges are included into Daymet but they are not adjusted for gauge undercatch by the wind. Daymet applies a weighted linear regression to adjust the gauge data for elevation changes.

First, the ECCC stations (Figs. 1) used have a complete set of daily data throughout the CTRL simulation period. Model outputs from the closest model grid points to the station locations were compared with the station data. We discuss these data with respect to the continental divide, which is also the border between British Columbia (BC) and Alberta (AB). Two stations were located on the western side of the continental divide (Golden and Kootenay) and four on the eastern side (Kananaskis, Pekisko, Banff and Calgary). The measured mean annual amount of precipitation was generally consistent with those of the CTRL simulation, with an average normalized bias of 5.3 % across all the stations. The bias varies from site to site. Simulated precipitation at Golden and Kootenay (Fig. 2) on the western side of the continental divide was underestimated (on average by -14 %), while precipitation was overall overestimated on the eastern side (on average by 15 %). The precipitation phase was well reproduced at Kootenay, but solid precipitation was underestimated at Golden and

Kananaskis probably because of a warm bias at Golden and less precipitation was simulated at Kananaskis.

Second, because rain-snow transition occurs at temperatures near-0^{o}C, simulated hourly occurrences of surface temperature between -2^{o}C and 2^{o}C were compared with the observations from three stations (Fig. 2). The mean annual bias of hourly occurrences was -9.3 h at Kootenay, -18.8 h at Banff, and -20.5 h at Calgary. Stewart et al. (2023) also found good agreement between the observations and the simulation within this range of temperatures at Calgary.

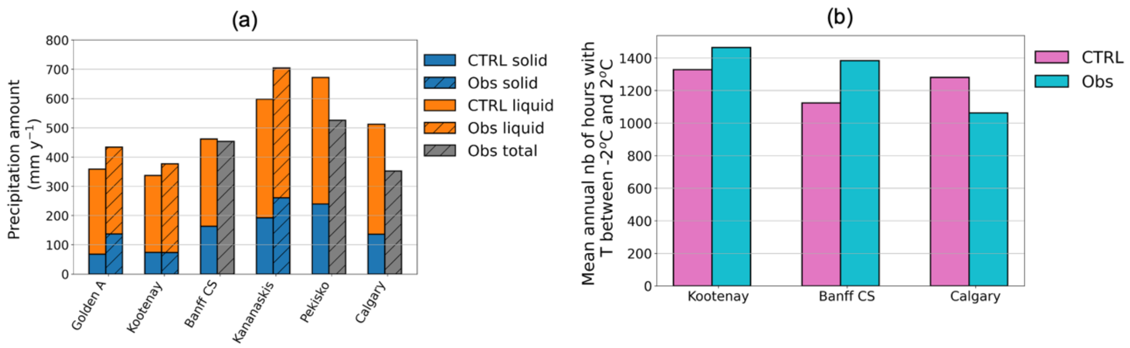

Figure 2. Comparison of the (a) average accumulated precipitation at the six stations (Fig. 1) using daily precipitation amounts and (b) of the hourly 2-m temperature occurrences at Kootenay, Banff CS and Calgary. These were the only stations with hourly 2-m temperature data.

Third, CTRL simulation output was compared to gridded precipitation and temperature from Daymet (Thornton et al., 2020) that had been upscaled from 1-km to 4-km grid-spacing (Fig. 3). Over the study domain (Fig. 1b), the bias of the mean annual accumulated precipitation between the CTRL and Daymet (CTRL-Daymet) over the 13 years was -68 mm, and the RMSE was 273 mm. The model well-reproduced the pattern and the values associated with the annual average 2-m temperature. The mean bias and RMSE for the mean daily 2-m temperature over the 13-years between the CTRL and Daymet were 0.02℃ and 1.02℃, respectively. Furthermore, the elevation-dependence bias was evaluated (not shown). The 2-m temperature bias decreases with increasing elevation. The median of the temperature bias remained within near-0^{o}C values, which are between -2^{o}C and 2^{o}C (Mekis et al. 2020). In contrast, the bias of average precipitation amounts increases with increasing elevation. This could be explained by the lack of observations at higher elevations (Lundquist et al. 2019), which could have resulted in a bias in the Daymet product.

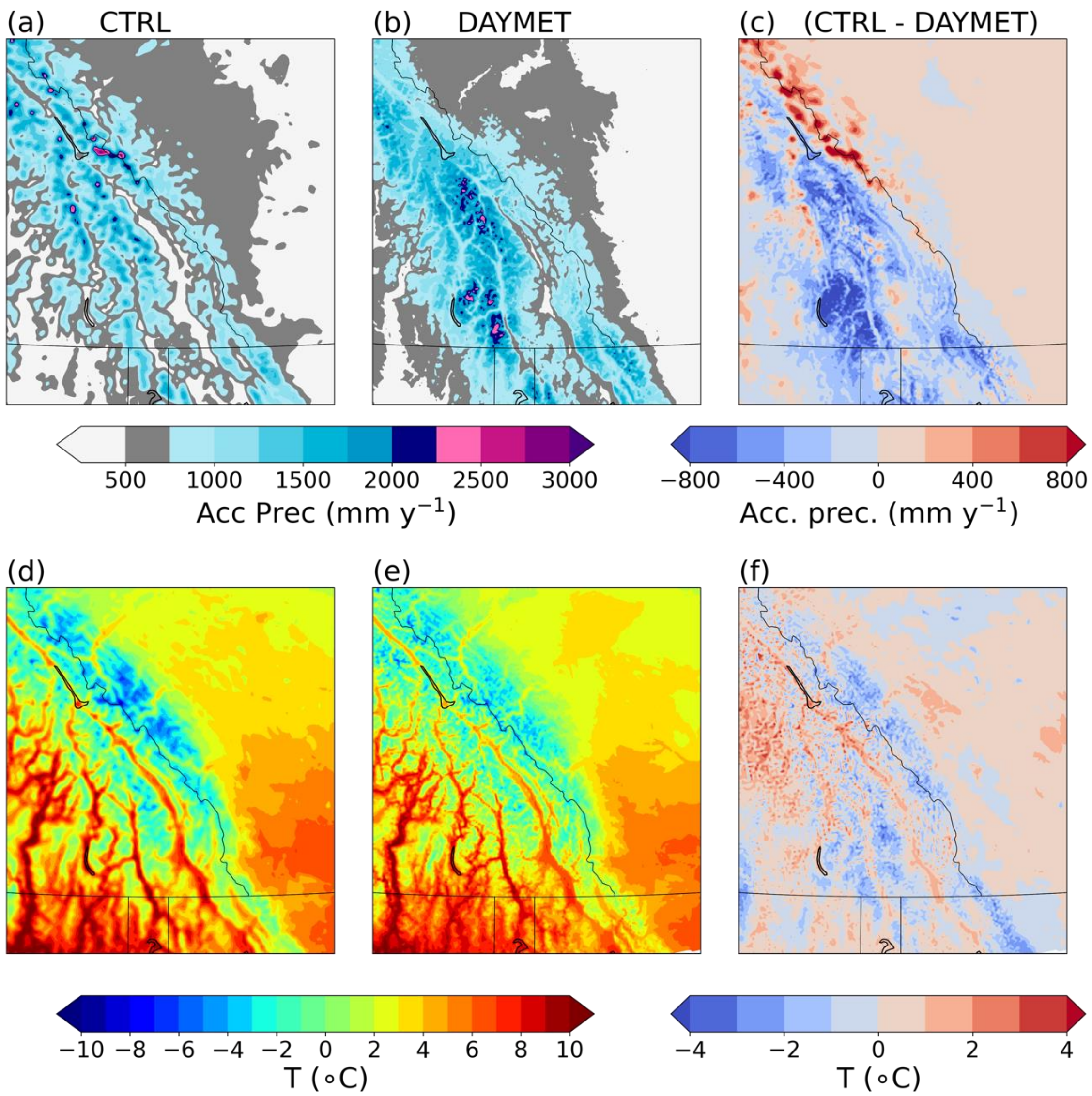

Figure 3. (a–c) Mean annual precipitation amounts between October 2000 and September 2013 produced by (a) the CTRL, (b) Daymet, and (c) the difference (CTRL–Daymet). (d–f) The mean daily 2-m temperature produced by (d) the CTRL, (e) Daymet, and (b and c) the difference (CTRL–Daymet). Note that the mean temperature in Daymet was obtained by averaging the minimum and maximum temperatures from the 13-year simulation.

To further assess the performance of the CTRL, Daymet was compared to ERA5-Land (Appendix A). Differences among the datasets were found, with biases that are higher than the bias between Daymet and CTRL. Our evaluation is similar to Henn et al. (2018). They compared multiple datasets over Western US, including Daymet. They found that most of them agree on the precipitation patterns but not on the annual amount of precipitation at higher elevations. Their analysis concluded that Daymet behaves within the range of uncertainties of other datasets over Western US. It is challenging to evaluate precipitation and temperature simulated by convection-permitting models over Canada because of the limited products available. Moreover, the evaluation of complex terrain with reliable data is also difficult. As pointed out by Lundquist et al. (2019), model results could be better for the precipitation patterns in mountainous terrain than observations because of the lack of stations at higher elevation.

To study the rain-snow transitions aloft, the simulated temperature structure was evaluated using atmospheric soundings. However, there is no sounding station in our domain, but we decided to use the closest one located near Edmonton, which is north of Calgary and farther east of the mountains. The CTRL simulation reproduced the measured height of the 0^{o}C isotherm quite well over Edmonton. The mean bias is -21.8 m, and the RMSE of 197.5 m.

Given the Liu et al. (2017)'s evaluation, the one by Almonte and Stewart (2019) as well as this current one, we believe it is appropriate to use the CTRL simulation in this study. Rain-snow transitions will be characterized using this dataset.

c. *Analysis of precipitation events*

A precipitation event was defined as consecutive hourly liquid-equivalent precipitation > 0.2 mm. ECCC defines the threshold value of 0.2 mm over a 24-h period to filter noise and other measurement errors. Given the models tend to produce high occurrences of low precipitation, it is necessary to use a threshold value (e.g. Di Luca et al. 2021). The 0.2 mm h^{-1} value produced a reasonable comparison with observations (e.g. Almonte and Stewart, 2019) and is between what has been used in other model studies (e.g. Di Luca et al. 2021 and Dai et al. 2017) and proposed by Kochendorfer et al. (2017), which is 0.5 mm h^{-1}. Precipitation events are separated by at least a 6-h continuous period without precipitation. Hence, if the interval between two precipitation episodes was less than 6 hours, the two episodes were treated as a single event.

Finally, simulated precipitation events were categorized based on the precipitation phase. They were divided into three categories: 1) rain; 2) mixed, including rain, snow, and graupel; and 3) solid, including snow and graupel. Precipitation events were computed using the model outputs at the six stations shown in Fig. 1.

d. *Analysis of the atmospheric conditions aloft*

The atmospheric conditions aloft associated with rain–snow transitions were characterized at two locations: Kootenay, BC and Calgary, AB (Fig. 1). Only two sites were chosen due to the higher computational capacity required to conduct the calculation over the full domain. The two sites are located on either side of the continental divide, at the same latitude, and are at approximately the same elevation (1151 m and 1063 m above sea level (ASL), respectively). Three parameters were calculated during rain and mixed precipitation events (Fig. 4).

First, the elevation of the 0°C isotherm (called 0°C level) was determined. The 0°C isotherm was determined by fitting a linear regression between the temperature and the associated elevation of two consecutive model levels. The height was determined using this linear regression if the function crossed 0°C. In the case of multiple 0°C levels, the highest level was kept because it is the level at which melting of solid precipitation could start. Mainly rain and mixed precipitation can reach the surface when considering only this level.

Second, because melting does not necessarily start at 0°C air temperature as it depends also on the relative humidity, the melting level, at which the wet-bulb temperature, T_w = 0°C, was calculated. This was determined to be the level at which solid precipitation, including graupel and snow, starts to melt. It also requires that the rain mixing ratio is > 0.005 g kg^{-1}.

Third, the level at which the solid precipitation has completely melted was determined. This corresponds to the lowest level of the rain–snow transition aloft (Fig. 4). A threshold of ice mixing ratio of 0.005 g kg^{-1}, including snow and graupel, was used to identify complete melting. At that level, only rain exists.

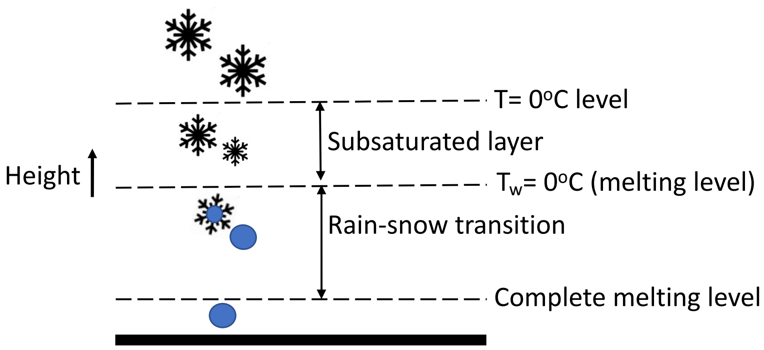

Figure 4. Schematic of the three parameters calculated using the WRF CONUS simulations to analyze the rain–snow transitions aloft. These parameters are the 0°C level, the melting level (T_w = 0°C), and the complete melting level. The sub-saturated layer is bound by the 0°C level and the melting level. The rain–snow transition is between the melting level and the complete melting level. Terminology is defined in the text.

The depth of the rain–snow transition aloft is defined by the vertical zone in which mixed precipitation exists. It is the difference between the melting level and the complete melting level (Fig. 4). Since precipitation often occurs in sub-saturated conditions over the Canadian Rockies, the difference between the 0°C level and the melting level can be large. The difference between those levels defines the depth of the sub-saturated warm layer. Note that, if precipitation was formed through a warm-rain process (e.g. Huffman and Norman, 1988) in the simulations, no melting level could be identified, and those precipitation events were excluded from the analysis.

e. Long-duration precipitation events

The atmospheric conditions that were present during long-duration precipitation events (> 24 h) at Kootenay and Calgary from October to June were identified to assess weather patterns. The sea level pressures, 500 hPa heights, as well as the vertically integrated moisture fluxes of the first hour of each long-duration event at both locations were averaged at each grid-point. The occurrences of 0°C aloft were also computed, with an emphasis on the phase transition period. As shown in Thériault et al. (2022), storms that reach either side of the divide can be formed from different types of weather systems.

3. Climatology of precipitation

The mean annual total precipitation, rainfall, snowfall, and graupel distributions were calculated from October 2000 to September 2013 using both CTRL and PGW simulations (Fig. 5). The total precipitation amounts were highly variable across the domain. In general, terrain at higher elevations received more precipitation than lower elevations due to orographic effects.

The highest amount of precipitation, which mostly occurred in the form of rain, was simulated on the western site of the divide (in BC). The maximum simulated amount was >3000 mm y^{-1}, while it was less, <1500 mm y^{-1}, on the eastern side. While this again highlights the orographic effects, precipitation amounts on each side of the divide can be reversed when the moisture flux comes from another direction (Thériault et al., 2022).

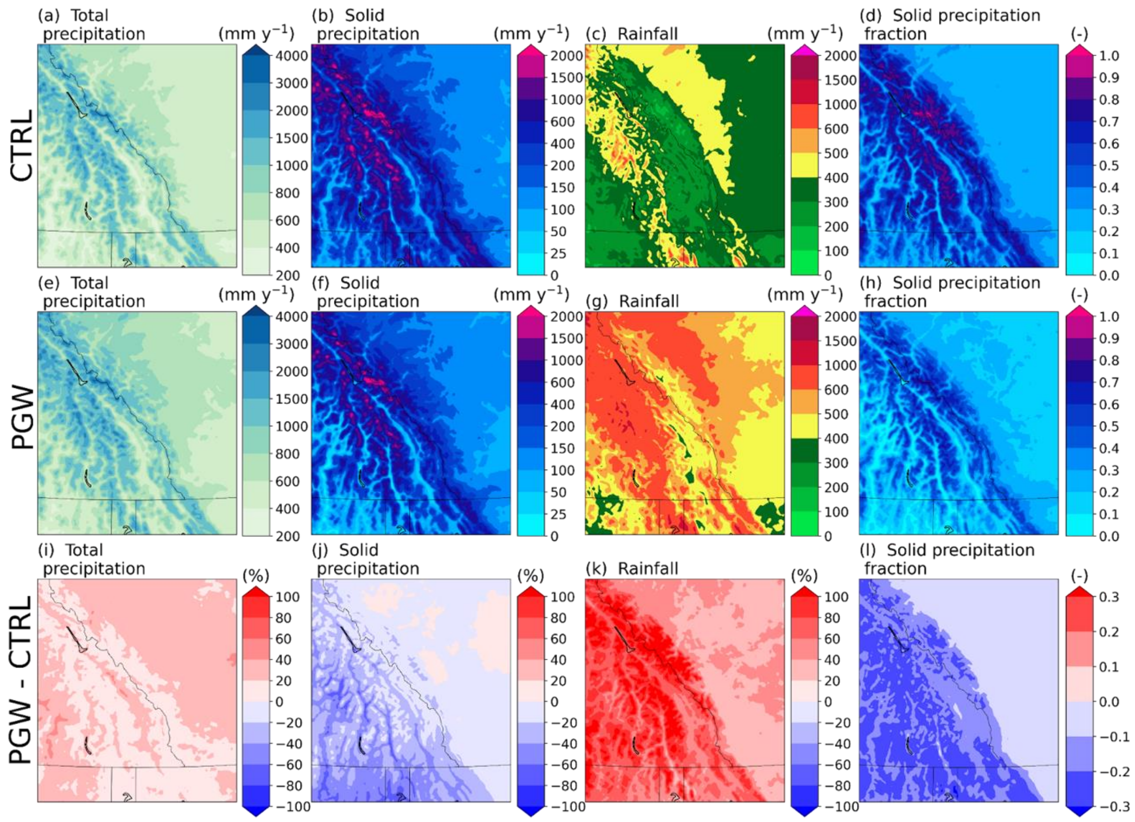

Figure 5. The 13-year average annual (a,e) total precipitation (mm y^{-1} in liquid equivalent), (b,f) solid precipitation (snowfall and graupel, mm y^{-1} in liquid equivalent), and (c,g) liquid precipitation (rainfall, mm y^{-1} in liquid equivalent) and (d,h) solid precipitation fraction (defined as the ratio of solid precipitation and total precipitation) using WRF–CTRL and WRF–PGW simulations. The difference (%) between the two simulations (PGW–CTRL) for annual (i) total precipitation, (j) solid precipitation (snowfall and graupel), (k) rainfall, and (l) solid precipitation fraction.

Both precipitation amounts and phase change in warmer conditions. Projected changes in the amount of total precipitation indicate an increase of up to 40–60% across the study area (Fig. 5). At higher elevations, the increase is less than 20%, while it is higher at lower elevations, including over the Canadian Prairies. There is also a large rainfall increase at lower elevations west of the continental divide. In contrast, solid precipitation indicates a decrease, particularly over the mountains west of the continental divide (Fig. 1). This is also shown by the solid precipitation fraction on Fig. 5. These numbers are consistent with the CMIP5 ensemble projection for the 2071–2100 period under RCP8.5 conditions (Liu et al. 2017).

4. Climatology of atmospheric conditions during rain–snow transitions

a. Historical climate

The occurrence of the 0°C level during rain and mixed precipitation was highly variable throughout the year for both Calgary and Kootenay (Fig. 6). Rain–snow transitions occurred most frequently in June at both locations (more than 300 occurrences), while they were the least frequent in February at both locations.

The range (25^{th} to 75^{th} percentile) of the 0°C level elevation (above sea level) was smaller in Kootenay than in Calgary. The largest range for the 0°C level, approximately 1.25 km, occurred in Calgary, from October to December. At Kootenay, the range was smaller by nearly 1 km in November and December, although it was only smaller by 0.25 km in October. The most extreme variations in the 0°C level (5^{th} to 95^{th} percentiles) occurred in May, September, and October in Calgary. Kootenay showed no clear tendency for 0°C-level variation, although the largest variations occurred in September and October.

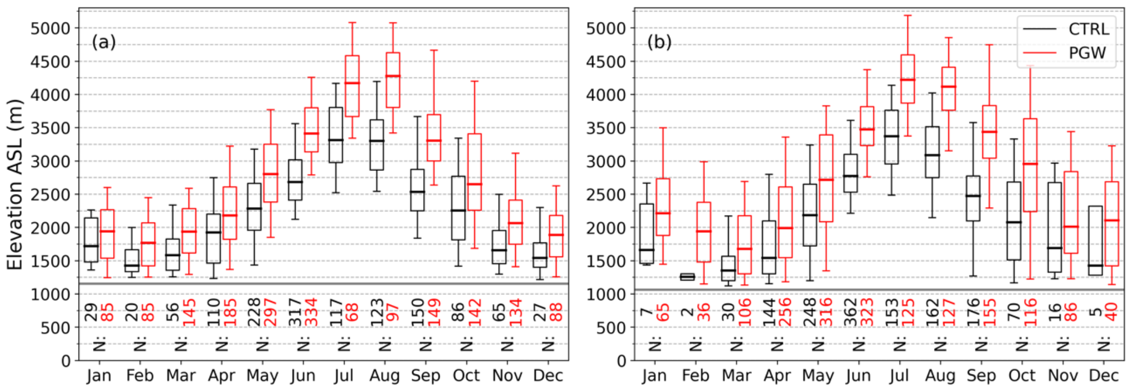

Figure 6. Boxplots of the elevation above sea level (ASL) of the 0°C level in the CTRL (black) and PGW (red) simulations for (a) Kootenay, BC and (b) Calgary, AB during rain or mixed precipitation events. Whiskers represent the 5th and 95th percentiles and the boxes are the 25th and 75th percentiles of the distributions. The number of occurrences (N) is shown along the x-axis.

The mean annual elevations in the 0°C level between the CTRL simulations for both locations were 2441 m ASL in Calgary and 2392 m ASL in Kootenay. The climate normal based on ECCC records shows that the mean diurnal surface temperature variation in Kootenay is approximately 10°C in November to January, while it is up to 13°C in Calgary. Despite the two meteorological stations being only 150-km apart, the Calgary area is influenced by larger temperature swings during winter. This could be due to strong downslope flow known as Chinook winds (MacDonald et. al., 2018), and the migration of artic air masses across the Prairies. Kochtubajda et al. (2017) showed that freezing rain, which is associated with a melting layer aloft, can be produced by the warm air lifting over the cold Arctic air mass over the Prairies. However, Chinook events are generally drier (MacDonald et al. 2018) with almost no precipitation.

A subsaturated layer is often present at the top of the melting layer aloft during rain and mixed precipitation events at both locations (Fig. 7). Although the median depth of the subsaturated layer is between 100 m and 300 m, the monthly range can exceed 800 m. This layer was present only a few times in Calgary during the fall and winter, which may be due to the fewer rain and mixed precipitation events. These subsaturated conditions can be associated with westerly flow and the Chinook winds that result in warm and dry conditions on the lee side of the Canadian Rockies.

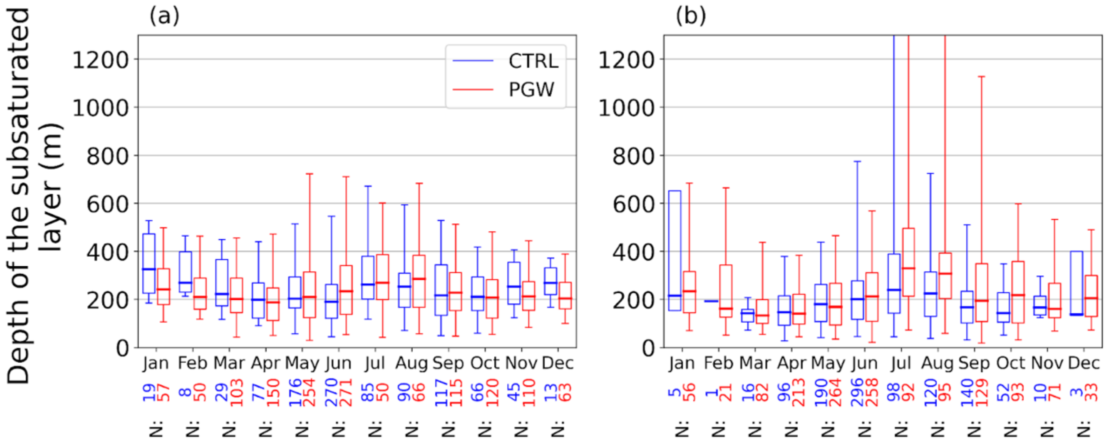

Figure 7. Boxplots of the depth of the subsaturated layer above the melting layer in the CTRL (blue) and PGW (red) simulations for (a) Kootenay, BC, and (b) Calgary, AB. The definition of this variable is given Fig. 4. Whiskers represent the 5^{th} and 95^{th} percentiles and the boxes are the 25th and 75th percentiles of the distributions. The number of occurrences (N) is shown along the x-axis.

The depths of the rain–snow transitions in Kootenay and Calgary are shown in Fig. 8. The rain–snow transition is deeper in Calgary than in Kootenay, at 384 m and 318 m on average, respectively. The median depth reached its maximum during the summer months (e.g., up to 482 m in July in Calgary and up to 422 m in August in Kootenay). It was generally deeper in Calgary from April to November. The depths of the rain–snow transition varied from 100 m to up to 1 km in July, which is also the month during which the 0°C level was highest, at almost 5 km (Fig. 6). The seasonal variation of the depth of the rain-snow transition could be associated with an increase in solid precipitation (mainly graupel) at the top of the rain-snow transition in the summer. This increase in solid precipitation would lead to slower melting rates and, in turn, deeper rain-snow transitions.

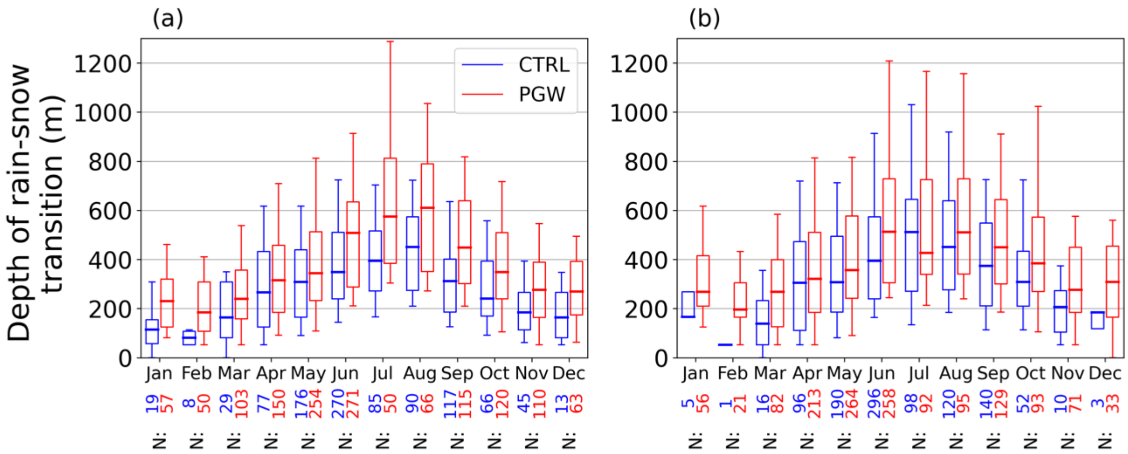

Figure 8. Boxplots of the depths of the rain–snow transitions in the CTRL (blue) and PGW (red) simulations for (a) Kootenay, BC, and (b) Calgary, AB. The definition of this variable is given Fig. 4. Whiskers represent the 5th and 95th percentiles and the boxes are the 25th and 75th percentiles of the distributions. The minimum and maximum values of the whiskers are the 5th and 95th percentiles, respectively. The number of occurrences (N) is shown along the x-axis.

b. Changes in warmer conditions

The temperature structure associated with the rain–snow transitions changed in warmer conditions using the PGW simulation. The changes were not uniform for Kootenay or Calgary.

The changes in the 0°C level are shown in Fig. 6. Both locations showed greater occurrences of a melting layer aloft in PGW conditions, except during the summer months. The difference between the CTRL and PGW simulations was greater during the winter compared to the spring. Although the number of occurrences varied throughout the year, the elevation of the 0°C level increased throughout the year for the PGW simulations (Fig. 6). For example, the monthly median 0°C level elevation increased between CTRL and PGW by 224 m (January) and 973 m (August) in Kootenay and by 324 m (March) and 1030 m (August) in Calgary. The mean annual variation in the 0°C level between the CTRL and PGW simulations was 74 m higher in Calgary (ranging from 2559 m to 2925 m ASL) compared to Kootenay (ranging from 2502 m to 2794 m ASL) throughout the year. Hence, the two locations are consistent with the more significant warming in Calgary than in Kootenay. At both locations, the increase of the median elevation of the 0°C level was greater (over 800 m) from July to October, and it was lower (under 500 m) from March to May, and in November.

The depth of the subsaturated layer at the top of the melting layer in PGW conditions remained somewhat constant in Kootenay, while it became generally thicker in Calgary (Fig. 7). Atmospheric conditions became drier in May and June in Kootenay, while drier conditions occurred from July to October in Calgary.

Finally, the average depth of the rain–snow transition is deeper at both locations (426 m and 371 m, respectively) and remained deeper in Calgary than in Kootenay in PGW conditions (Fig. 8). The depth of the rain-snow transition probably increases for a similar reason than for the deeper rain-snow transition in the summer in CTRL. The top of the rain-snow transition increases, and that level is associated with higher solid precipitation amounts. The higher solid precipitation amount, including more graupel, would melt slower and, in turn, would produce deeper rain-snow transitions.

5. Atmospheric conditions during precipitation events

a. Distribution of precipitation events

The distribution of rain, mixed precipitation and snow events varied between sites (Fig. 9). In the CTRL simulations, there were more rain events than snow events at all six locations. The number of mixed precipitation events was almost constant, at approximately 40 events, with most events lasting less than 2 h. The western side of the continental divide had more rain events than the eastern side, except in Calgary. Other stations had about 20 fewer rain events than in Calgary. Banff experienced the highest number of snow events. Kananaskis experienced very long events, up to 80 h, which could have been associated with mixed precipitation.

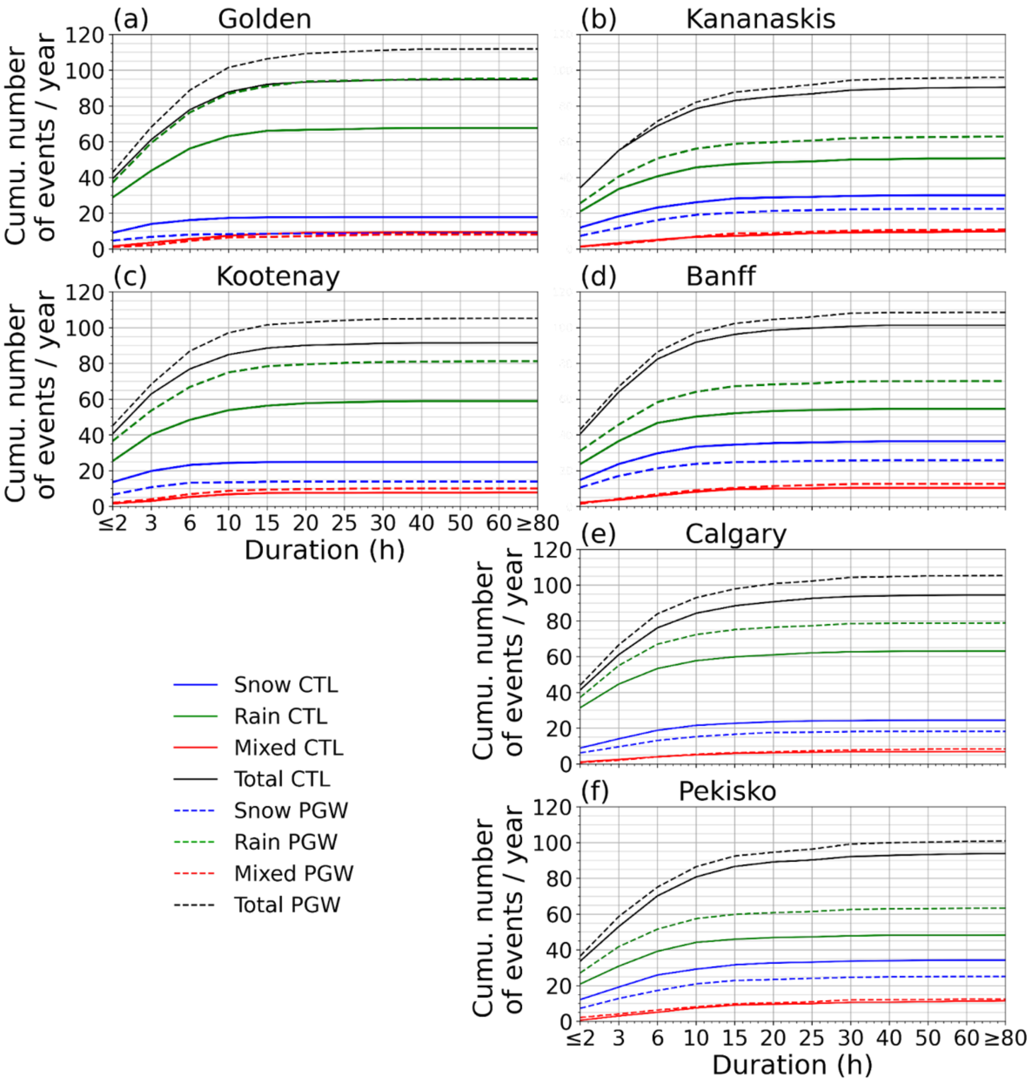

Figure 9. Cumulated number of mean annual of solid precipitation (snow and graupel) events, mixed precipitation (rain, snow, and graupel), rain events, and total events between 2000 and 2013 at six stations in the Canadian Rockies in both CTRL and PGW.

Based on the simulations, the distribution of events is expected to change in warmer conditions. Total number of events increases in warmer conditions. They tend to increase more on the western side (up to 20 events) compared to the eastern side (up to 10 events). The relative number of rain events increases at all sites while the number of snow events decrease due to the increase of the elevation of the 0°C level aloft. The number of mixed precipitation events remains mainly unchanged in PGW. Some of the snow events evolved into mixed precipitation.

b. *Atmospheric conditions in long-duration events*

We investigated atmospheric conditions for long-duration events in Kootenay and Calgary. A composite map of all the long-duration precipitation events that occurred during the simulation period (CTRL only) was produced (Fig. 10). Eight events were determined at Kootenay (5 rain and 3 mixed) and 22 events at Calgary (8 rain, 7 mixed and 7 snow).

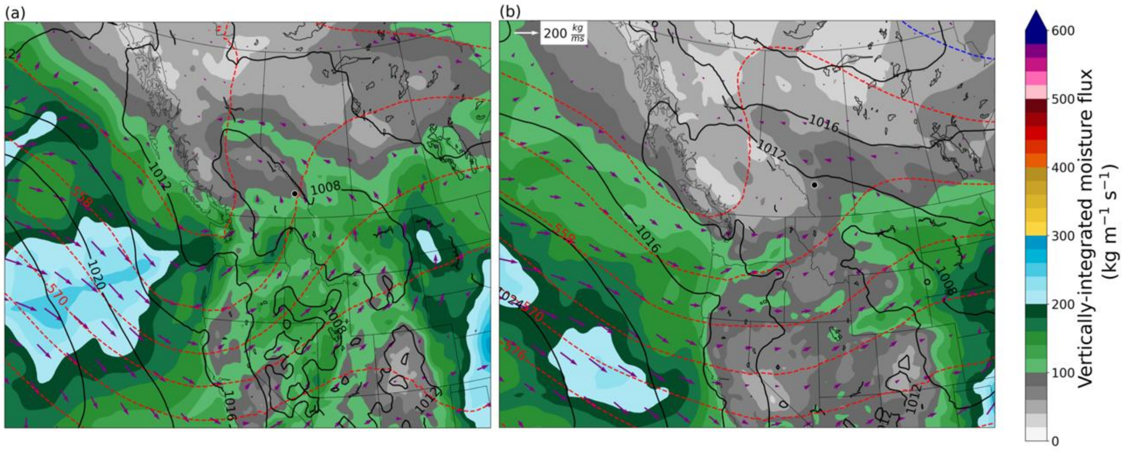

Figure 10. Composite atmospheric conditions during long-duration events in (a) Kootenay, BC and (b) Calgary, AB. Sea level pressure isobars (black contours) and 500-hPa geopotential height isohypses (blue and red dashed contours). Shading and purple arrows represent the magnitude and direction of vertically integrated moisture fluxes, respectively. The atmospheric conditions were averaged at each grid point at the onset of precipitation. Eight events were used at Kootenay and 22 events at Calgary were used for the composite maps.

Despite both the Calgary and Kootenay stations being located relatively close to each other (~150 km), the composite map of synoptic patterns associated with long-duration events show major differences. For Calgary, the composite shows a typical pattern associated with lee-side cyclogenesis leading to easterly upslope flow over the eastern slopes of the Canadian Rockies. This synoptic-scale pattern is similar to that of the June 2013 Calgary flood (Liu et al., 2016; Milrad et al., 2015; Pomeroy et al., 2016), which is one of the long-duration events identified at both Calgary and Kootenay. In contrast, the composite for Kootenay shows low IVT over the site with a general southwesterly moisture flow to the south of it. The upper-level trough is located farther west (trough axis at around 130 °W) than for Calgary. This is because the stronger pressure gradient at the surface and aloft over the eastern Pacific Ocean produces a strong eastward moisture flux. Six of the seven events are associated with easterly flows on the eastern slope of the Canadian Rockies during the long-precipitation events at Kootenay. The other event was associated with atmospheric river landfall. Overall, this suggests that westerly flows from the Pacific Ocean can lead to long-duration precipitation events in Kootenay without reaching Calgary. In contrast, lee-side cyclogenesis can lead to long-duration events on both sides of the continental divide (e.g. Liu et al. 2016; Flesch & Reuter, 2012).

The associated vertical temperature structure depends on which side of the continental divide is being considered (Fig. 11). For precipitation events identified in Kootenay, the environmental air was warmer east of the continental divide. In contrast, precipitation events at Calgary were associated with colder atmospheric conditions on the eastern side. The 0°C level is at approximately 1500 m ASL near the eastern slope of the Canadian Rockies leading to a rain-snow transition at the surface (Minder et al. 2011).

While precipitation events in Calgary were all associated with similar weather patterns, this was not the case in Kootenay. It was, however, not possible to associate a weather pattern with the characteristic of the rain-snow transition aloft because they occur from October to June. Most of the rain events at both Kootenay and Calgary occurred in June (10 and 13 events, respectively), are associated with lee-cyclogenesis and an elevation of the 0ºC level of around 2500 m ASL and higher. The other events occurred during relatively colder months, such as November, April, and May, so the 0°C level was generally lower (up to 2500 m ASL). The event associated with the lowest 0°C level diagnosed (up to 2000 m ASL) at Kootenay and Calgary were associated with moisture coming from the Pacific Ocean but from different directions and at different times during the year (Kootenay was in November and Calgary in April). The moisture flux leading to the precipitation in Kootenay was southwesterly and reached Kootenay while it was northwesterly for the Calgary event and travelled south eastward to cycle back over the Prairies to reach the eastern side of the Canadian Rockies.

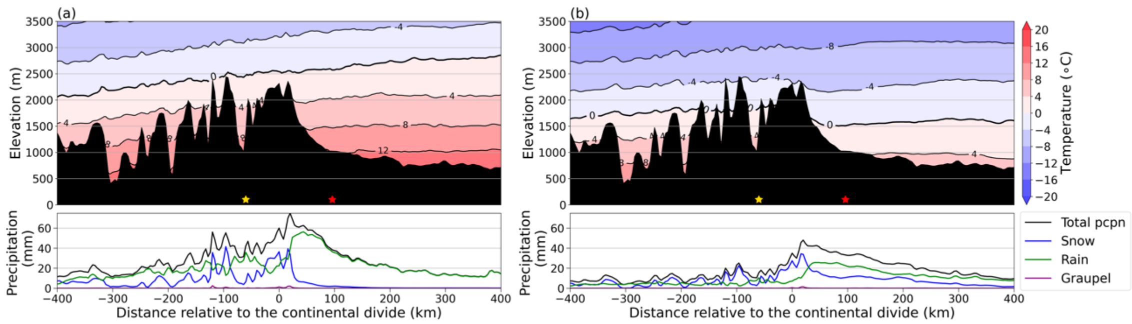

Figure 11. Composite temperature (shading) and precipitation cross-section during long-duration events in (a) Kootenay, BC and (b) Calgary, AB. Amounts of total precipitation (black), snow (blue), rain (green), and graupel (purple) are shown. The yellow star indicates the location of Kootenay, and the red star indicates Calgary.

These findings differ from those of the 2019 SPADE project (Thériault et al. 2022). No long-duration precipitation event associated with moisture flow from the Pacific Ocean were documented during SPADE. But, precipitation that crossed the divide and originating from lee-side cyclogenesis was observed. Sharma & Déry (2020) suggested that most atmospheric river landfalls occur in September and October, which is a different period than studied in SPADE. Further analyses are needed to better understand weather patterns leading to precipitation crossing the continental divide when the moisture comes from the Pacific Ocean.

6. Summary and conclusions

Our study investigated the changes in conditions associated with near-0°C temperatures that can lead to rain–snow transitions. We examined the 0°C level, the presence of a subsaturated layer at temperatures greater than 0°C, and rain–snow transitions aloft in the western Canadian mountains, near the continental divide. The WRF 4-km simulations from 2000–2013 in both historical and future conditions were used. Our analysis led to the following conclusions.

- A melting layer aloft with rain or mixed precipitation can occur throughout the year over the Canadian Rockies. These occurrences are expected to increase in future warmer conditions, particularly in winter, on the eastern side of the continental divide (Calgary). The depth of the subsaturated layer and the rain–snow transitions will change in the warmer conditions, but this change is somewhat different between Kootenay and Calgary.

- The PGW simulations predict that the mean height of the 0°C level during rain or mixed precipitation will increase by 276 m and 346 m in Kootenay and Calgary, respectively, compared to the CTRL values. The greatest increases in elevation are predicted to occur between July and October at both locations. This isotherm is expected to reach mean elevations of 2668 m asl and 2787 m asl in Kootenay and Calgary, respectively.

- Synoptic-scale conditions during which long-duration rain–snow transitions (> 24 h) occurred were different depending on whether the event occurred on the western or eastern side of the continental divide. No long-duration events occurred on both sides of the divide simultaneously. Furthermore, during the Calgary flooding event in 2013, a long-precipitation event was simulated in

Calgary but not Kootenay.

There are some limitations to this study. While the PGW method can demonstrate a realistic thermodynamic response to global warming, it can only simulate minimal changes for large-scale atmospheric circulation. The variables used for the three-dimensional analysis (such as mixing ratios, temperature aloft, geopotential height) were only available at 3-hour intervals, compared to the hourly data that were available for surface precipitation fields. This may lead to an underestimation of the occurrence of short-duration events (< 3 h). The elevations at which the melting processes started and stopped were approximated to the nearest vertical levels of the model, which are not necessarily at regular spacings (hybrid levels). The linear interpolation used to estimate the height of the 0°C isotherm could have led to some errors in the calculation. Both these issues introduce some uncertainty to the computed variables when characterizing the precipitation transitions aloft. In addition, it is recognized that further analyses should be conducted on the weather and other factors leading to the features of rain-snow transitions aloft that were examined in this study, including studies on the effect of Chinook and atmospheric rivers over the west coast.

Overall, this study illustrates critical features of the complex atmospheric conditions aloft in connection with rain–snow transitions across the continental divide in the southern Canadian Rockies. Large variations in the current and future climates were demonstrated, associated with moisture aloft and not just temperature. These variations were shown to greatly influence the types of precipitation that occurred at the surface. In turn, these precipitation types cause a host of issues related to the development and evolution of the snowpack (e.g. Musselman et al. 2017) and the degree to which flooding, and avalanches occur.

Acknowledgements

The research was supported in part by Mountain Water Futures, funded by the Canada First Research Excellence Funds (CFREF) Global Water Futures (GWF), a NSERC Discovery grant and the Canada Research Chair Program (CRC-2018-00312). This research was enabled in part by support provided by Calcul Québec (www.calculquebec.ca) and Compute Canada (www.computecanada.ca). We would like to thank Julien Chartrand and Sébastien Marinier for contributing to some of the initial analyses as well as the anonymous reviewers to their constructive comments. The WRF HRCONUS dataset is available at https://rda.ucar.edu/datasets/ds612.0/. Data from the ECCC meteorological stations used can be found at https://climate.weather.gc.ca/historical_data/search_historic_data_e.html.

Appendix A

Liu et al. (2016) have performed an evaluation of the simulations mainly over the Continental United States. Given that our study region is located in southern Canada, additional evaluation of the temperature and the precipitation has been performed.

A1. Evaluation of the precipitation amount

Precipitation from Daymet (Thornton et al. 2020) and ERA5-Land (Hersbach et al. 2020) were compared against each other and to the CTRL simulation (Figs. A1). The bias varies with the data dataset used for comparison. ERA5-Land underestimates annual precipitation amounts compared to CTRL and Daymet; the biases are, respectively, -29.4 mm and -89.6 mm, whereas Daymet overestimates precipitation amounts produced by CTRL, with a bias of 68.1 mm. Between all products, the root mean square error (RMSE) are all within the same values, which vary from 223.4 mm to 273 mm.

To compare ERA5-Land with Daymet, Daymet was upscaled to a grid-spacing of 9 km (Fig. A1). The bias over the study area between ERA5-Land and Daymet is the largest (-89.6 mm). From Fig. A1, ERA5-Land is slightly wetter over the Prairies and in the valleys and drier over most of the mountainous regions. The largest difference is west of the continental divide in the Purcell mountains. In contrast, the CTRL simulation is wetter over the Prairies with respect to ERA5-Land and in the mountainous regions. Finally, the CTRL simulation is also wetter than Daymet over the Prairies, drier over the Purcell mountains, and wetter in the north side of Canadian Rockies.

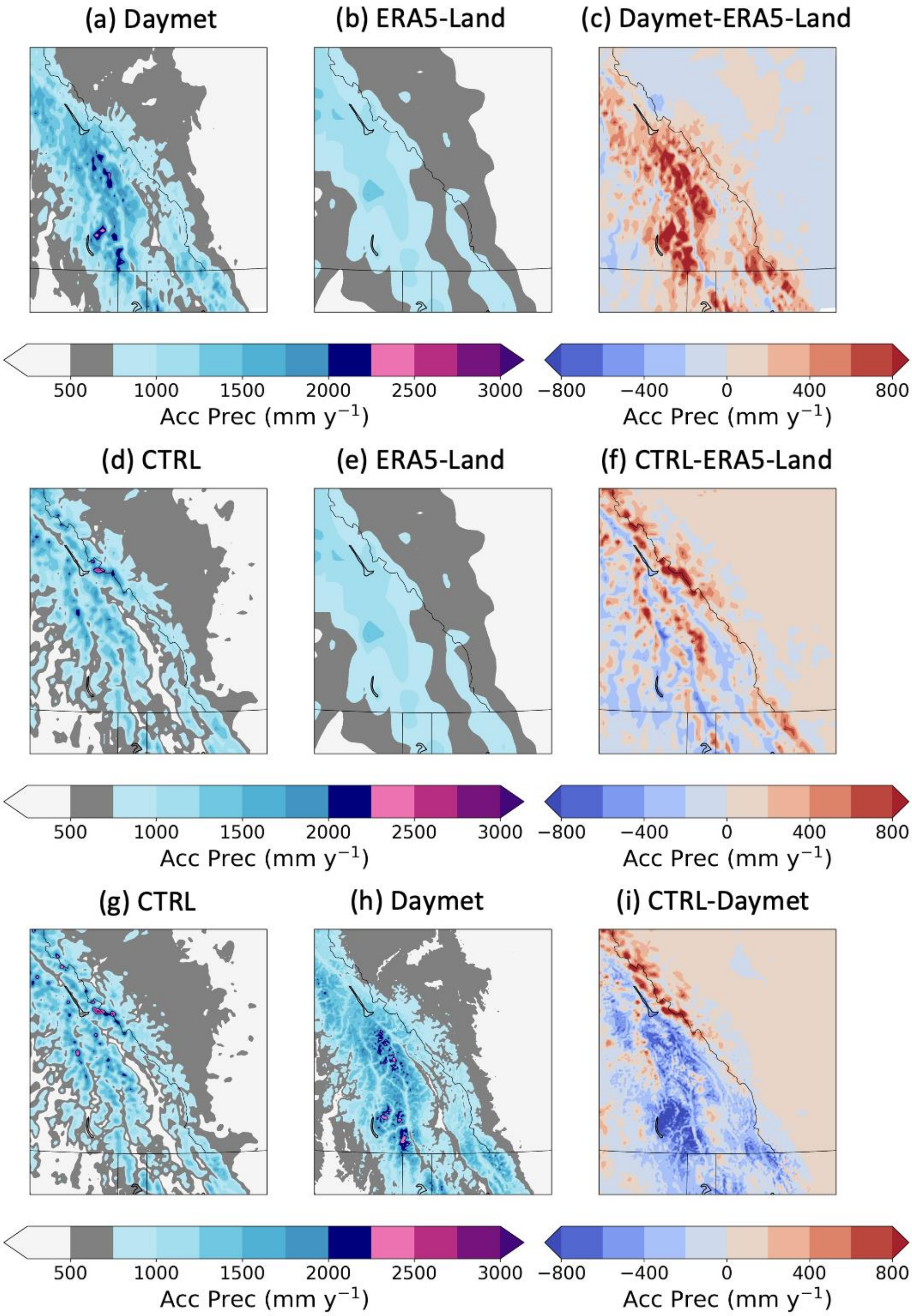

Figure A1: Average total annual precipitation amount between 2000-2013 from the (a) Daymet, (b) ERA5-Land and (c) Daymet - ERA5-Land. Daymet was upscaled to the grid-spacing of ERA5-Land, which is 9 km. (d-f) are the comparison between CTRL and ERA5-Land. The resolution of the CTRL was upscaled to the same as ERA5-Land (9 km grid-spacing). (g-i) are the comparison between CTRL and Daymet. Daymet was upscaled to 4 km grid-spacing as CTRL.

The precipitation patterns are overall the same, but Daymet features more details than ERA5-Land (9 km) in the amount of precipitation due to the fine spatial grid-spacing of 1 km; this is particularly obvious in the mountains. When focusing over our study region, the bias between CTRL and ERA5-Land is lower (in absolute value) than between DAYMET and ERA5-Land. However, each dataset has their limitations. While ERA5-Land is a reanalysis hourly product, it is at coarser resolution compared to Daymet, which is a daily product, at much finer resolution.

A2. Evaluation of the 2-m temperature

The 2-m air daily average temperature from Daymet was compared with ERA5-Land over the study area (Fig. A2). Daymet was again upscaled to the resolution of ERA5-Land. Daymet is generally warmer than ERA5-Land over the mountains and slightly colder over the Prairies. The overall daily bias is, however, only 0.4^{o}C. The temperature bias is similar between the CTRL and ERA5-Land (0.4^{o}C, Fig. A2) but the bias between CTRL and Daymet is lower (0.01^{o}C). The RMSE between Daymet and ERA5-Land and CTRL and ERA5-Land were identical at 1.5 ^{o}C, while it is only 1^{o}C between CTRL and Daymet. As for the precipitation comparison, the bias and RMSE of CTRL-Daymet were lower than between the ERA5-Land and Daymet, giving us confidence in the simulation.

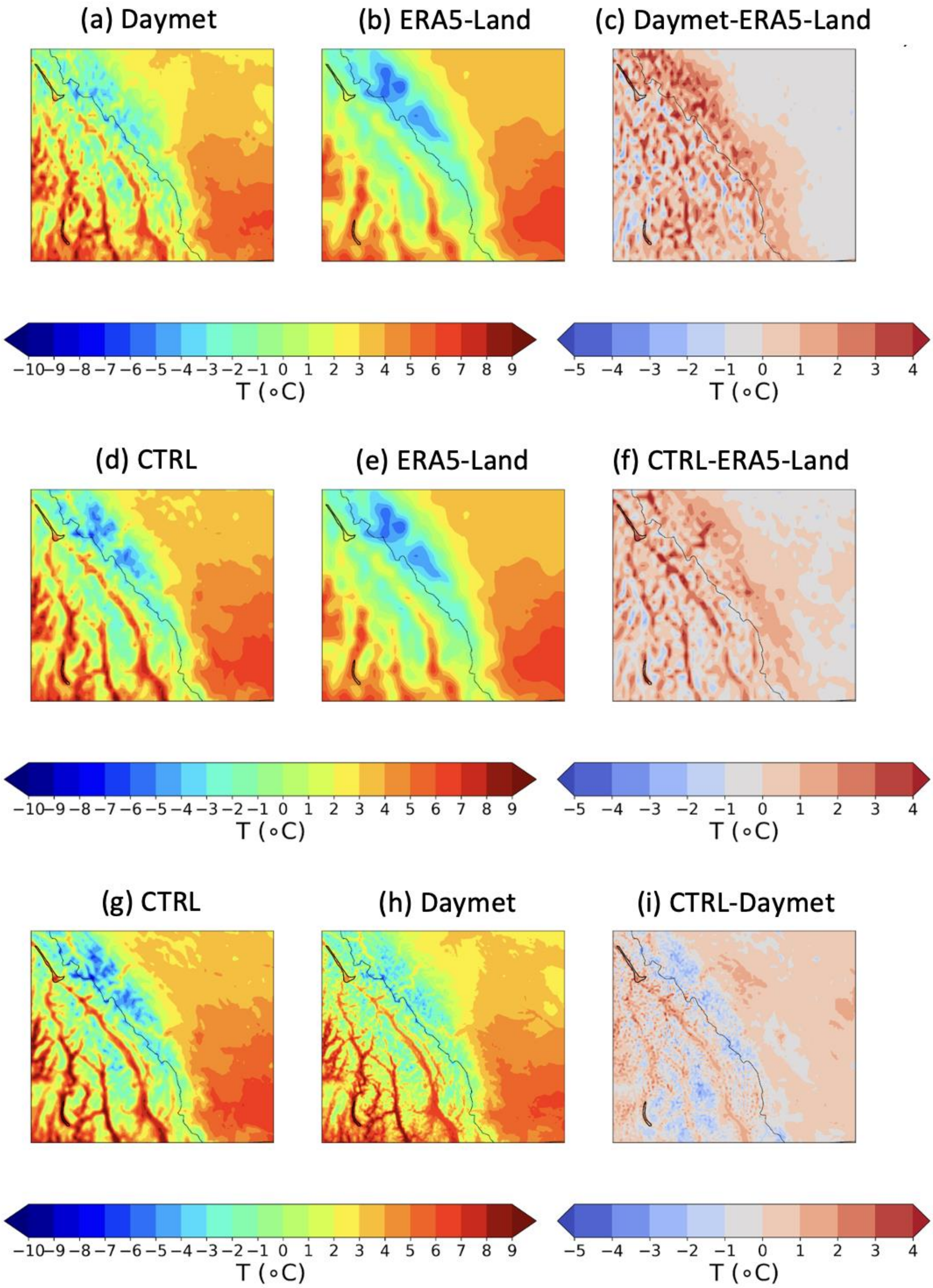

Figure A2: Same as Fig. A1 but for the 2-m air temperature.

References

Almonte, J. D., & Stewart, R. E. (2019). Precipitation transition regions over the southern Canadian Cordillera during January–April 2010 and under a pseudo-global-warming assumption. *Hydrology and Earth System Sciences*, *23*(9), 3665–3682. https://doi.org/10.5194/hess-23-3665-2019

Dai, A., Rasmussen, R.M., Liu, C. & co-authors (2020) A new mechanism for warm-season precipitation response to global warming based on convection-permitting simulations. *Climate Dynamics*, 55, 343–368. https://doi.org/10.1007/s00382-017-3787-6

Di Luca, A., Argüeso, D., Sherwood, S., & Evans, J. P. (2021) Evaluating precipitation errors using the environmentally conditioned intensity-frequency decomposition method. *Journal of Advances in Modeling Earth Systems*, 13, e2020MS002447. https://doi.org/10.1029/2020MS002447

DeBeer, C. M., Wheater, H. S., Carey, S. K., & Chun, K. P. (2016). Recent climatic, cryospheric, and hydrological changes over the interior of western Canada: A review and synthesis. *Hydrology and Earth System Sciences*, *20*(4), 1573–1598. https://doi.org/10.5194/hess-20-1573-2016

DeBeer, C. M., Wheater, H. S., Pomeroy, J. W., Barr, A. G., Baltzer, J. L., Johnstone, J. F., Turetsky, M. R., Stewart, R. E., Hayashi, M., van der Kamp, G., Marshall, S., Campbell, E., Marsh, P., Carey, S. K., Quinton, W. L., Li, Y., Razavi, S., Berg, A., McDonnell, J. J., Pietroniro, A. (2021). Summary and synthesis of Changing Cold Regions Network (CCRN) research in the interior of western Canada – Part 2: Future change in cryosphere, vegetation, and hydrology. *Hydrology and Earth System Sciences*, *25*(4), 1849–1882. https://doi.org/10.5194/hess-25-1849-2021

Flesch, T. K., & Reuter, G. W. (2012). WRF Model Simulation of two Alberta flooding events and the impact of topography. *Journal of Hydrometeorology*, *13*(2), 695–708. https://doi.org/10.1175/JHM-D-11-035.1

Guan, B., Waliser, D. E., Ralph, F. M., Fetzer, E. J., & Neiman, P. J. (2016). Hydrometeorological characteristics of rain-on-snow events associated with atmospheric rivers. *Geophysical Research Letters*, *43*(6), 2964–2973.

Kochendorfer, J., Nitu, R., Wolff, M., Mekis, E., Rasmussen, R., Baker, B., Earle, M. E., Reverdin, A., Wong, K., Smith, C. D., Yang, D., Roulet, Y.-A., Buisan, S., Laine, T., Lee, G., Aceituno, J. L. C., Alastrué, J., Isaksen, K., Meyers, T., Brækkan, R., Landolt, S., Jachcik, A., and Poikonen, A.: Analysis of single-Alter-shielded and unshielded measurements of mixed and solid precipitation from WMO-SPICE, Hydrol. Earth Syst. Sci., 21, 3525–3542, https://doi.org/10.5194/hess-21-3525-2017, 2017.https://doi.org/10.1002/2016GL067978

Hägeli, P., & McClung, D. M. (2003). Avalanche characteristics of a transitional snow climate—Columbia Mountains, British Columbia, Canada. *Cold Regions Science and Technology*, *37*(3), 255–276. https://doi.org/10.1016/S0165-232X(03)00069-7

Hanesiak, J. M., Stewart, R. E., Bonsal, B. R., Harder, P., Lawford, R., Aider, R., Amiro, B. D., Atallah, E., Barr, A. G., Black, T. A., Bullock, P., Brimelow, J. C., Brown, R., Carmichael, H., Derksen, C., Flanagan, L. B., Gachon, P., Greene, H., Gyakum, J., Zha, T. (2011). Characterization and summary of the 1999–2005 Canadian Prairie drought. *Atmosphere-Ocean*, *49*(4), 421–452. https://doi.org/10.1080/07055900.2011.626757

Harder, P., & Pomeroy, J. (2013). Estimating precipitation phase using a psychrometric energy balance method: Precipitation phase using a psychrometric energy balance. *Hydrological Processes*, *27*(13), 1901–1914. https://doi.org/10.1002/hyp.9799

Hersbach, H, Bell, B, Berrisford, P, & al. (2020). The ERA5 global reanalysis. Quaterly Journal Royal Meteorological Society, 146, 1999– 2049. https://doi.org/10.1002/qj.3803

Henn, B., A. J. Newman, B. Livneh, C. Daly, &J. D. Lundquist (2018). An assessment of differences in gridded precipitation datasets in complex terrain, *Journal of Hydrology*, 556, 1205-1219. https://doi.org/10.1016/j.jhydrol.2017.03.008.

Huffman, G. J., &G. A. Norman Jr . (1988) The supercooled warm rain process and the specification of freezing precipitation. *Monthly Weather Review*, 116, 2172–2182. doi:10.1175/1520-0493(1988)116<2172:TSWRPA>2.0.CO;2.

Kochtubajda, B., Stewart, R. E., Boodoo, S., Thériault, J. M., Li, Y., Liu, A., Mooney, C., Goodson, R., & Szeto, K. (2016). The June 2013 Alberta catastrophic flooding event - part 2: Fine-scale precipitation and associated features: Precipitation and Associated Features of the 2013 Alberta Flood. *Hydrological Processes*, *30*(26), 4917–4933. https://doi.org/10.1002/hyp.10855

Kochtubajda, B., C. Mooney & R. Stewart (2017). Characteristics, atmospheric drivers and occurrence patterns of freezing precipitation and ice pellets over the Prairie Provinces and Arctic Territories of Canada: 1964–2005, *Atmospheric Research*, 191, 115-127. https://doi.org/10.1016/j.atmosres.2017.03.005.

Kochendorfer, J., Nitu, R., Wolff, M., Mekis, E., Rasmussen, R., Baker, B., Earle, M. E., Reverdin, A., Wong, K., Smith, C. D., Yang, D., Roulet, Y.-A., Buisan, S., Laine, T., Lee, G., Aceituno, J. L. C., Alastrué, J., Isaksen, K., Meyers, T., Brækkan, R., Landolt, S., Jachcik, A., and Poikonen, A. (2017). Analysis of single-Alter-shielded and unshielded measurements of mixed and solid precipitation from WMO-SPICE, *Hydrol. Earth Syst. Sci.*, 21, 3525–3542, https://doi.org/10.5194/hess-21-3525-2017, 2017.

Liu, A. Q., Mooney, C., Szeto, K., Thériault, J. M., Kochtubajda, B., Stewart, R. E., Boodoo, S., Goodson, R., Li, Y., & Pomeroy, J. (2016). The June 2013 Alberta catastrophic flooding event: Part 1-Climatological aspects and hydrometeorological features: Climatological aspects and hydrometeorological features. *Hydrological Processes*, *30*(26), 4899–4916. https://doi.org/10.1002/hyp.10906

Liu, C., Ikeda, K., Rasmussen, R., Barlage, M., Newman, A. J., Prein, A. F., Chen, F., Chen, L., Clark, M., Dai, A., Dudhia, J., Eidhammer, T., Gochis, D., Gutmann, E., Kurkute, S., Li, Y., Thompson, G., & Yates, D. (2017). Continental-scale convection-permitting modeling of the current and future climate of North America. *Climate Dynamics*, *49*(1–2), 71–95. https://doi.org/10.1007/s00382-016-3327-9

Lundquist, J., Hughes, M., Gutmann, E., & Kapnick, S. (2019). Our skill in modeling mountain rain and snow is bypassing the skill of our observational networks. *Bulletin of the American Meteorological Society*, *100*(12), 2473–2490. https://doi.org/10.1175/BAMS-D-19-0001.1

MacDonald, M. K., J. W. Pomeroy & R. L.H. Essery (2018). Water and energy fluxes over northern prairies as affected by chinook winds and winter precipitation, *Agricultural and Forest Meteorology*, 248, 372-385. https://doi.org/10.1016/j.agrformet.2017.10.025.

Milrad, S. M., Gyakum, J. R., & Atallah, E. H. (2015). A meteorological analysis of the 2013 Alberta flood: Antecedent large-scale flow pattern and synoptic–dynamic characteristics. *Monthly Weather Review*, *143*(7), 2817–2841. https://doi.org/10.1175/MWR-D-14-00236.1

Minder, J. R., Letcher, T. W., & Liu, C. (2018). The character and causes of elevation-dependent warming in high-resolution simulations of Rocky Mountain climate change. *Journal of Climate*, *31*(6), 2093–2113. https://doi.org/10.1175/JCLI-D-17-0321.1

Musselman, K., Clark, M., Liu, C. et al. (2017) Slower snowmelt in a warmer world. *Nature Climate Change* 7, 214–219. https://doi.org/10.1038/nclimate3225

Pomeroy, J. W., Stewart, R. E., & Whitfield, P. H. (2016). The 2013 flood event in the south Saskatchewan and Elk river basins: Causes, assessment and damages. *Canadian Water Resources Journal / Revue Canadienne Des Ressources Hydriques*, *41*(1–2), 105–117. https://doi.org/10.1080/07011784.2015.1089190

Radić, V., Cannon, A. J., Menounos, B., & Gi, N. (2015). Future changes in autumn atmospheric river events in British Columbia, Canada, as projected by CMIP5 global climate models. *Journal of Geophysical Research: Atmospheres*, *120*(18), 9279–9302. https://doi.org/10.1002/2015JD023279

Sankaré, H., & Thériault, J. M. (2016). On the relationship between the snowflake type aloft and the surface precipitation types at temperatures near 0°C. *Atmospheric Research*, *180*, 287–296. https://doi.org/10.1016/j.atmosres.2016.06.003

Sharma, A. R., & Déry, S. J. (2020). Contribution of atmospheric rivers to annual, seasonal, and extreme precipitation across British Columbia and southeastern Alaska. *Journal of Geophysical Research: Atmospheres*, *125*(9). https://doi.org/10.1029/2019JD031823

Shepherd, T. G. (2014). Atmospheric circulation as a source of uncertainty in climate change projections. *Nature Geoscience*, *7*(10), 703–708. https://doi.org/10.1038/ngeo2253

Stewart, R. E., Liu, Z., Thériault, J. M., & Ruman, C. J. (2023). The occurrence of near-0°C surface air temperatures in the current and pseudo-global warming future over southern Canada. *Journal of Geophysical Research: Atmospheres*, 128, e2022JD037981.

Teufel, B., Diro, G. T., Whan, K., Milrad, S. M., Jeong, D. I., Ganji, A., Huziy, O., Winger, K., Gyakum, J. R., de Elia, R., Zwiers, F. W., & Sushama, L. (2017). Investigation of the 2013 Alberta flood from weather and climate perspectives.

Climate Dynamics, *48*(9–10), 2881–2899. https://doi.org/10.1007/s00382-016-3239-8

Thériault, J. M., Hung, I., Vaquer, P., Stewart, R. E., & Pomeroy, J. W. (2018). Precipitation characteristics and associated weather conditions on the eastern slopes of the Canadian Rockies during March–April 2015. *Hydrology and Earth System Sciences*, *22*(8), 4491–4512. https://doi.org/10.5194/hess-22-4491-2018

Thériault, J. M., *N. R. Leroux, R. E. Stewart, A. Bertoncini, S. J. Déry, J. W. Pomeroy, *H. D. Thompson, *H. Smith, Z. Mariani, *A. Desroches-Lapointe, S. Mitchell, and *J. Almonte. (2022). Storms and precipitation across the continental divide experiment (SPADE). *Bulletin of the American Meteorological Society*.[In Press]

Thompson, G., & Eidhammer, T. (2014). A study of aerosol impacts on clouds and precipitation development in a large winter cyclone. *Journal of the Atmospheric Sciences, 71*(10), 3636–3658. https://doi.org/10.1175/JAS-D-13-0305.1

Thornton, M.M., Shrestha, R., Wei, Y., Thornton, P.E., Kao, S., & Wilson, B.E. (2020). *DaymetDaymet: Monthly Climate Summaries on a 1-km Grid for North America, Version 4* [NetCDF, GTiff]. 0 MB. https://doi.org/10.3334/ORNLDAAC/1855

Wallace, B., & Minder, J. R. (2021). The impact of snow loss and soil moisture on convective precipitation over the Rocky Mountains under climate warming. *Climate Dynamics*, *56*(9–10), 2915–2939. https://doi.org/10.1007/s00382-020-05622-7

Whitfield, P. H., & Pomeroy, J. W. (2016). Changes to flood peaks of a mountain river: Implications for analysis of the 2013 flood in the Upper Bow River, Canada: Changes Affecting Flood Peaks of Upper Bow River. *Hydrological Processes*, *30*(25), 4657–4673. https://doi.org/10.1002/hyp.10957

Figure captions

Figure 1. Location of the study area. (a) Domain of the simulations including the topography and the cross section (red line) along which temperature and precipitation were analyzed (Section 5b) and (b) the sub-domain of interest. The meteorological stations used in this study are indicated by the black dots. The elevation of each station and the closest model grid point (in parentheses) are Banff: 1396.9 m (1579.9 m), Calgary: 1081.9 m (1078.2 m), Fernie: 1001.0 m (1199.2 m), Golden: 784.9 m (922.5 m), Kananaskis: 1391.1 m (1474.4 m), Kootenay: 935.0 m (1150.9 m) and Pekisko: 1415.0 m (1509.9 m).

Figure 2. Comparison of the (a) average accumulated precipitation at the six stations (Fig. 1) using daily precipitation amounts and (b) of the hourly 2-m temperature occurrences at Kootenay, Banff CS and Calgary. These were the only stations with hourly 2-m temperature data.

Figure 3. (a–c) Mean annual precipitation amounts between October 2000 and September 2013 produced by (a) the CTRL, (b) Daymet, and (c) the difference (CTRL–Daymet). (d–f) The mean daily 2-m temperature produced by (d) the CTRL, (e) Daymet, and (b and c) the difference (CTRL–Daymet). Note that the mean temperature in Daymet was obtained by averaging the minimum and maximum temperatures from the 13-year simulation.

Figure 4. Schematic of the three parameters calculated using the WRF CONUS simulations to analyze the rain–snow transitions aloft. These parameters are the 0°C level, the melting level (T_w = 0°C), and the complete melting level. The sub-saturated layer is bound by the 0°C level and the melting level. The rain–snow transition is between the melting level and the complete melting level. Terminology is defined in the text.

Figure 5. The 13-year average annual (a,e) total precipitation (mm y^{-1} in liquid equivalent), (b,f) solid precipitation (snowfall and graupel, mm y^{-1} in liquid equivalent), and (c,g) liquid precipitation (rainfall, mm y^{-1} in liquid equivalent) and (d,h) solid precipitation fraction (defined as the ratio of solid precipitation and total precipitation) using WRF–CTRL and WRF–PGW simulations. The difference (%) between the two simulations (PGW–CTRL) for annual (i) total precipitation, (j) solid precipitation (snowfall and graupel), (k) rainfall, and (l) solid precipitation fraction.

Figure 6. Boxplots of the elevation above sea level (ASL) of the 0°C level in the CTRL (black) and PGW (red) simulations for (a) Kootenay, BC and (b) Calgary, AB during rain or mixed precipitation events. Whiskers represent the 5th and 95th percentiles and the boxes are the 25th

and 75th percentiles of the distributions. The number of occurrences (N) is shown along the x-axis.

Figure 7. Boxplots of the depth of the subsaturated layer above the melting layer in the CTRL (blue) and PGW (red) simulations for (a) Kootenay, BC, and (b) Calgary, AB. The definition of this variable is given Fig. 4. Whiskers represent the 5^{th} and 95^{th} percentiles and the boxes are the 25th and 75th percentiles of the distributions. The number of occurrences (N) is shown along the x-axis.

Figure 8. Boxplots of the depths of the rain–snow transitions in the CTRL (blue) and PGW (red) simulations for (a) Kootenay, BC, and (b) Calgary, AB. The definition of this variable is given Fig. 4. Whiskers represent the 5^{th} and 95^{th} percentiles and the boxes are the 25th and 75th percentiles of the distributions. The minimum and maximum values of the whiskers are the 5^{th} and 95^{th} percentiles, respectively. The number of occurrences (N) is shown along the x-axis.

Figure 9. Cumulated number of mean annual of solid precipitation (snow and graupel) events, mixed precipitation (rain, snow, and graupel), rain events, and total events between 2000 and 2013 at six stations in the Canadian Rockies in both CTRL and PGW.

Figure 10. Composite atmospheric conditions during long-duration events in (a) Kootenay, BC and (b) Calgary, AB. Sea level pressure isobars (black contours) and 500-hPa geopotential height isohypses (blue and red dashed contours). Shading and purple arrows represent the magnitude and direction of vertically integrated moisture fluxes, respectively. The atmospheric conditions were averaged at each grid point at the onset of precipitation. Eight events were used at Kootenay and 22 events at Calgary were used for the composite maps.

Figure 11. Composite temperature (shading) and precipitation cross-section during long-duration events in (a) Kootenay, BC and (b) Calgary, AB. Amounts of total precipitation (black), snow (blue), rain (green), and graupel (purple) are shown. The yellow star indicates the location of Kootenay, and the red star indicates Calgary.

Figure A1: Average total annual precipitation amount between 2000-2013 from the (a) Daymet, (b) ERA5-Land and (c) Daymet - ERA5-Land. Daymet was upscaled to the grid-spacing of ERA5-Land, which is 9 km. (d-f) are the comparison between CTRL and ERA5-Land. The resolution of the CTRL was upscaled to the same as ERA5-Land (9 km grid-spacing). (g-i) are the comparison between CTRL and Daymet. Daymet was upscaled to 4 km grid-spacing as CTRL.

Figure A2: Same as Fig. A1 but for the 2-m air temperature.